

Robust Active Shape Model Search

Mike Rogers and Jim Graham

Division of Imaging Science and Biomedical Engineering, University of Manchester,
mike.rogers@man.ac.uk,
<http://www.isbe.man.ac.uk/~mdr/personal.html>

Abstract. Active shape models (ASMs) have been shown to be a powerful tool to aid the interpretation of images. ASM model parameter estimation is based on the assumption that residuals between model fit and data have a Gaussian distribution. However, in many real applications, specifically those found in the area of medical image analysis, this assumption may be inaccurate. Robust parameter estimation methods have been used elsewhere in machine vision and provide a promising method of improving ASM search performance. This paper formulates M-estimator and random sampling approaches to robust parameter estimation in the context of ASM search. These methods have been applied to several sets of medical images where ASM search robustness problems have previously been encountered. Robust parameter estimation is shown to increase tolerance to outliers, which can lead to improved search robustness and accuracy.

Keywords. Medical Image Understanding, Shape, Active Shape Models, Robust Parameter Estimation, M-estimators, RANSAC, Weighted Least Squares.

1 Introduction

Statistical shape models have been shown to be a powerful tool to aid the interpretation of images. Models represent the shape and variation of object classes and can be used to impose *a-priori* constraints on image search. A frequently used formulation, on which we shall concentrate in this paper, is the Active Shape Model (ASM) [3], which also provides a method of fitting the model to image data. ASMs have been applied to many image analysis tasks, most successfully when the object class of interest is fairly consistent in shape and gray-level appearance [3][13][16]. The technique can suffer from a lack of robustness when image evidence is noisy or highly variable [2][10]. Many medical images display these types of characteristics.

To fit a model to data, parameters must be estimated in an optimal manner. Standard ASM parameter estimation minimises the sum of squares of residuals between the model and the data. It has been widely recognised that least squares minimisation only yields optimal results when the assumption of Gaussian distributed noise is met. Under real conditions a Gaussian model of residual distribution is seldom accurate. Least squares estimation is especially sensitive

to the presence of gross errors, or outliers [5]. Medical images containing widely varying appearance and detailed structure potentially give rise to non-Gaussian residuals, including outliers, breaking down the assumptions upon which ASM parameter estimation is built. Robust methods of parameter estimation provide a promising method of increasing the accuracy and robustness of ASM search.

Many computer vision problems are related to estimating parameters from noisy data. Robust minimisation techniques have been applied to many areas of machine vision. Torr and Murray [17] compare methods for the calculation of the Fundamental Matrix, the calibration-free representation of camera motion. Robust techniques have also been used in conic fitting [19], cartography [4], tracking [1] and registration [20].

In this paper we investigate the case of robust parameter estimation techniques for shape-model fitting. We use ASM search as a paradigm for shape fitting, although the methods may be applied using any other parameterisation of shape. We formulate several robust parameter estimation schemes and present a quantitative comparison of the methods against standard least squares parameter estimation using several sets of medical images. The image sets have been chosen because ASM search has previously been found to be insufficiently robust in locating object boundaries.

1.1 Statistical Shape Models

Here we describe briefly the shape models used to represent deformable object classes. ASMs are built from a training set of annotated images, in which corresponding points have been marked. The points from each image are represented as a vector \mathbf{x} after alignment to a common co-ordinate frame [3]. Eigen-analysis is applied to the aligned shape vectors, producing a set of *modes of variation* \mathbf{P} . The model has parameters \mathbf{b} controlling the shape represented as:

$$\mathbf{x} = \bar{\mathbf{x}} + \mathbf{P}\mathbf{b} \quad (1)$$

where $\bar{\mathbf{x}}$ is the mean aligned shape. The shape \mathbf{x} can be placed in the image frame by applying an appropriate pose transform.

Neglecting alignment, the process of estimating model parameters \mathbf{b} for a given shape \mathbf{x} proceeds by minimising the residuals:

$$\mathbf{r} = (\mathbf{x} - \mathbf{x}_0) \quad (2)$$

where \mathbf{x}_0 is the current reconstruction of the model. Least squares estimation therefore seeks to minimise $E_1(\mathbf{b}) = \mathbf{r}^T \mathbf{r}$, specifically we wish to find $\delta\mathbf{b}$ so as to minimise $E_1(\mathbf{b} + \delta\mathbf{b})$. This can be shown to have a solution of the form:

$$\delta\mathbf{b} = (\mathbf{P}^T \mathbf{P})^{-1} \mathbf{P}^T \delta\mathbf{x} \quad (3)$$

which, as \mathbf{P} is orthonormal, simplifies to:

$$\delta\mathbf{b} = \mathbf{P}^T \delta\mathbf{x}. \quad (4)$$

This is the standard ASM parameter update equation for iterative search [3] and as such is expected to operate in the presence of noise in the shape update vector $\delta\mathbf{x}$. The estimator is optimal with respect to a Gaussian noise model. In the presence of non-Gaussian noise the estimator is suboptimal, specifically a single outlying value can significantly distort model parameters by an arbitrary amount.

In ASM search, the update vector $\delta\mathbf{x}$ is obtained by searching the local image area around each landmark point. Models of local image appearance for each landmark point are built from the training set. These are used at each iteration of search to determine the best local landmark position.

2 Robust Parameter Estimation

There are many robust estimation techniques in the literature [4][5][7][12][15][18]. For the purposes of ASM parameter estimation, they can be divided into two categories: M-estimators and random sampling techniques, which we describe in the following sections.

2.1 M-Estimators

The aim of M-estimators is to alter the influence of outlying values to make the distribution conform to Gaussian assumptions. The estimators minimise the sum of a symmetric positive definite function:

$$\min \sum_i \rho(r_i). \quad (5)$$

where r_i is the i th element of the residual vector $\mathbf{r} = (r_1, r_2, \dots, r_n)$.

The M-estimator of \mathbf{b} based on the function $\rho(r_i)$ is the solution to the following m equations:

$$\sum_i \psi(r_i) \frac{\partial r_i}{\partial b_j} = 0, \text{ for } j = 1, \dots, m, \quad (6)$$

where the derivative $\psi(x) = d\rho(x)/dx$ is called the influence function, representing the the influence of a datum on the value of the parameter estimate. A weighting function is defined as:

$$\omega(x) = \frac{\psi(x)}{x} \quad (7)$$

and (6) becomes:

$$\sum_i \omega(r_i) r_i \frac{\partial r_i}{\partial b_j} = 0, \text{ for } j = 1, \dots, m. \quad (8)$$

which is a weighted least squares problem. In the ASM formulation $\partial\mathbf{r}/\partial\mathbf{b}$ is given by \mathbf{P} , resulting in a solution with the form:

$$\delta \mathbf{b} = \mathbf{K}^T \delta \mathbf{x} \quad (9)$$

where $\mathbf{K} = (\mathbf{P}^T \mathbf{W}^T \mathbf{W} \mathbf{P})^{-1} \mathbf{P}^T \mathbf{W}^T \mathbf{W}$ and \mathbf{W} is a diagonal matrix formed from the weights ω_i .

Weighting Strategies. There are many possible forms for the function $\rho(x)$, a summary is given in [19]. Each is designed to weight the influence of residuals under non-Gaussian conditions. One of the most consistent and widely used forms was devised by Huber [7], which results in a weighting function of:

$$\omega_i = \begin{cases} 1 & r_i < \sigma \\ \sigma/|r_i| & \sigma \leq r_i < 3\sigma \\ 0 & r_i \geq 3\sigma \end{cases} \quad (10)$$

where σ is an estimate of the standard deviation of the residuals. The standard deviation σ is not known, but can be robustly estimated from the median of the absolute values of the residuals [12]:

$$\sigma = 1.4826(1 + 5/(n - p))\text{median}|r_i| \quad (11)$$

where n is the number of data points and p is the length of the parameter vector.

Equations 10 and 11 allow the calculation of a set of weights, which can be applied in Eqn. 9 to calculate model parameter updates. This process must be iterated to convergence with re-weighting at each stage to form a final parameter estimate. We will refer to this weighted least squares method as WLS Huber.

In ASM search, profile models are used to generate the update shape vector $\delta \mathbf{x}$, by searching local image regions. The positions at which image data has the smallest Mahalanobis distance d from the profile models are chosen as the new landmarks for model parameter estimation. Bearing this in mind, an alternative weighting scheme can be devised for ASM model fitting that draws on the likelihoods of profile matches. Mahalanobis distance d is distributed as a χ^2 with $(p - 1)$ degrees of freedom, where p is the number of parameters of the profile model, and can therefore be used to generate a probability for each element of \mathbf{x} given the model in the standard way. These probabilities \mathbf{p} , one for each element of \mathbf{x} , can be used directly in a weighted least squares estimator. This estimator reflects the quality of the image evidence from which the data resulted, rather than the spatial distribution of points from which the model parameters are to be estimated. We refer to this as WLS Image.

2.2 Random Sampling

Random sample based robust parameter estimation is, in some sense, the opposite approach to the smoothing effect of least squares and iterated weighted least squares. Rather than maximising the amount of data used to obtain an initial solution and then identifying outliers, as small a subset of the data as is feasible is used to estimate model parameters. This process is repeated enough times to

ensure that within a some level of probability at least one of the subsets will contain only good data.

One of the first robust estimation algorithms was random sample consensus (RANSAC), introduced by Fischler and Bolles [4]. RANSAC proceeds by selecting random subsets of data and evaluating them in terms of the amount of data that is consistent with the resulting model parameterisation. After a certain number of trails, the parameters with the largest *consensus set* is accepted as the parameter estimate. A threshold can be set to stop the algorithm when an acceptable consensus has been achieved. In order to determine the consensus set, a distance measure between model and data points must be defined, together with a threshold on this value.

In the case of ASMs, parameter estimation from random subsets of data can easily be achieved by a weighted least squares scheme with binary weights. The size of the consensus set can be determined by thresholding residual values after model reconstruction in the image co-ordinate system.

A later example of a random sampling algorithm was least median of squares (LMedS), proposed by Rousseeuw [12]. LMedS estimates model parameters by minimising the non-linear function:

$$\text{median} \mathbf{r}^T \mathbf{r}. \quad (12)$$

The algorithm is in fact extremely similar to RANSAC, the major differences being that LMedS does not require a consensus threshold, and unlike RANSAC no threshold is defined to end further random sampling.

In both algorithms we would ideally like to consider every possible subset of the data. This is usually infeasible, so methods are required to calculate the largest number of subsets required to guarantee a subset containing only good data. Assuming the proportion of outliers in the data is ϵ , the probability that at least one of m subsets consists of only good data is given by:

$$\gamma = 1 - (1 - (1 - \epsilon)^p)^m \quad (13)$$

where p is the size of each subset. If $\gamma \rightarrow 1$, then

$$m = \frac{\log(1 - \gamma)}{\log(1 - (1 - \epsilon)^p)} \quad (14)$$

In practice ϵ must be estimated by an educated worst guess of the proportion of outliers. Commonly $\gamma \geq 0.95$. We note that LMedS is computationally inefficient in the presence of Gaussian noise [12] as a fixed number of parameter estimations are always carried out. Both RANSAC and LMedS can be optimised for specific tasks [20].

We note that other random sampling algorithms exist in the literature, for example: least trimmed squares [11], MINPRAM [14] and MLESAC [18]¹. These techniques have not been evaluated here because they are closely related to

¹ For a review of random sampling techniques see [8].

RANSAC and LMedS. For application to ASM parameter estimation, it is expected that any suitable random sampling robust parameter estimation algorithm will produce similar results to RANSAC or LMedS.

3 Experiments

To test the effects of using a robust ASM parameter estimation technique on image interpretation, we have carried out a set of experiments on three difference image sets. The image sets we have chosen are: electron microscope images of diabetetic nerve capillaries [10], Echocardiograms of the left ventricle [6] and magnetic resonance images (MRI) of the prostate [2]. Each set has been chosen because of the poor performance achieved using ASM interpretation in previous studies. Each type of image presents its own set of problems which must be addressed to achieve optimal interpretation results. Details of the training data available for each data set and the various modifications to the standard ASM algorithm are as follows:

- **Capillaries.** The training set consists of 33 electron microscope images digitised at 575×678 pixel 8-bit grey-scale. Each image has been annotated at the basement membrane/endothelial cell boundary up to 4 times by an expert on separate occasions, giving a set of 131 annotations. There is a large amount of ambiguity in the position of desired boundary, caused in part by locally consistent but confusing image evidence, resulting in considerable variability in expert-placed landmarks. A smoothed version of each annotated boundary has been represented by 50 evenly spaced landmark points. For this data, ASM profile models consist of a two cluster mixture model, where one cluster represents normal profile appearance and one for the locally confusing evidence. The two classes of profile appearance have been selected manually. The images are extremely complex and variable. Wavelet texture analysis has been applied to the images to remove some of this complexity. The ASM model built for this set of data has been found to impose only weak constraints due to the small amount of consistent structure in the capillary boundary shapes [9]. Figure 1 shows examples of these images.
- **Left Ventricle Echocardiograms.** The training set consists of 64 echocardiogram images digitised at 256×256 pixel 8-bit grey-scale. Each image has been expertly annotated with a plausible position of the left ventricle boundary. The boundaries have been represented by 100 evenly spaced landmarks. Echocardiogram images are inherently noisy and structural delineations are often poorly defined. ASMs have previously been applied to this data set using a genetic algorithm search technique [6] that identified many ambiguous possible model fit positions. Figure 2 shows some examples from this data.
- **Prostate.** This training set consists of 95 T2 weighted MRI images of the prostate and surrounding tissues at differing anterior depths, digitised at 256×256 pixel 8-bit grey scale. Annotations of the perimeter of the prostate

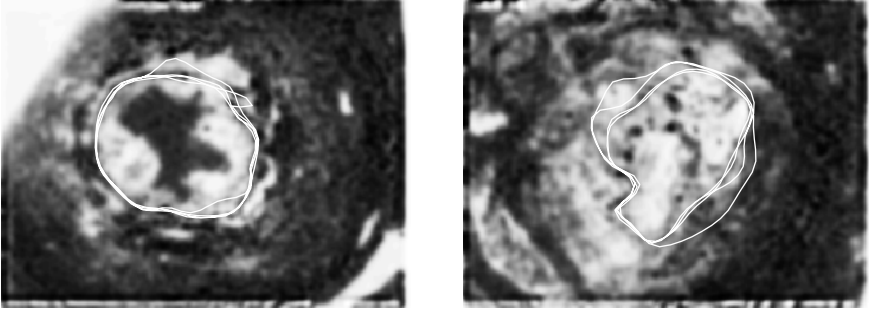


Fig. 1. Example capillary texture images with multiple ambiguous expert annotations.



Fig. 2. Example echocardiogram images with left ventricle boundary marked.

gland, consisting of 27 manually positioned landmarks, were used to train the ASM. There is significant variation in the structure and appearance of the tissue surrounding the prostate as the depth of the image slice varies. This has been found to adversely affect ASM search [2]. Figure 3 shows some examples from this data set.

On each image set we have evaluated several robust parameter estimation methods in terms of robustness and accuracy: simple least squares (LS), weighted least squares using Huber's iterated scheme (WLS Huber), weighted least squares with weights obtained directly from the image data (WLS Image), RANSAC and LMedS.

3.1 Random Sampling Subset Size

Before we can apply a random sampling technique to ASM parameter estimation, we must determine the smallest subset size that is feasible to instantiate the model parameters. There is no precise fixed method of directly determining

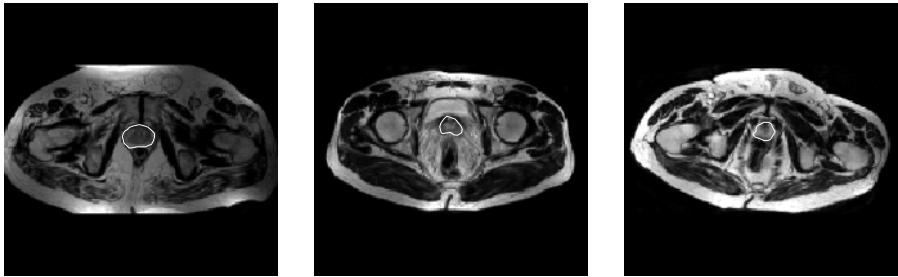


Fig. 3. Example prostate images with prostate perimeter marked.

this value. Rather, we can tune the subset size to achieve a certain accuracy whilst avoiding degenerate matrices. When constructing an ASM, the number of modes kept can be chosen to ensure that the model's training set is represented to a given accuracy [3]. A similar approach can be taken to determine the random subset size. A model's training set can be reconstructed using a RANSAC or LMedS approach with varying subset size and the corresponding residuals recorded. The random subset size can then be chosen to give a desired reconstruction accuracy, bearing in mind that larger subsets require far more random trials to ensure the same probability of considering a good subset.

Table 1 shows RANSAC training set reconstruction errors for a model built with 133 capillary boundaries. The table also shows the number of trails required to obtain a 95% probability of the good subset under the assumption that 10% of data is outlying.

Table 1. RANSAC training set reconstruction error for varying subset size. p is the proportion of the total landmark points in each subset, \bar{r} is the mean reconstruction residual in pixels across the entire training set and m is the number of trials required to obtain a good subset with 95% certainty under the assumption of $\epsilon = 10\%$.

p	\bar{r}	m
0.3	5.51	12
0.4	2.40	23
0.5	1.74	40
0.6	1.24	69
0.7	1.00	118
0.8	0.95	201
0.9	0.90	341

In the following evaluations we have chosen RANSAC and LMedS subset sizes of 0.4, 0.3 and 0.8 for capillary, left ventricle echocardiogram and prostate images respectively.

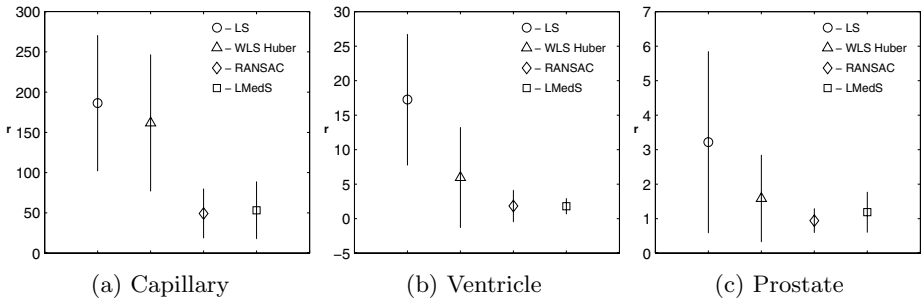


Fig. 4. Outlier tolerance for each set of data. Mean residual r over model training set perturbed by non-Gaussian noise. Error bars show ± 1 std. dev.

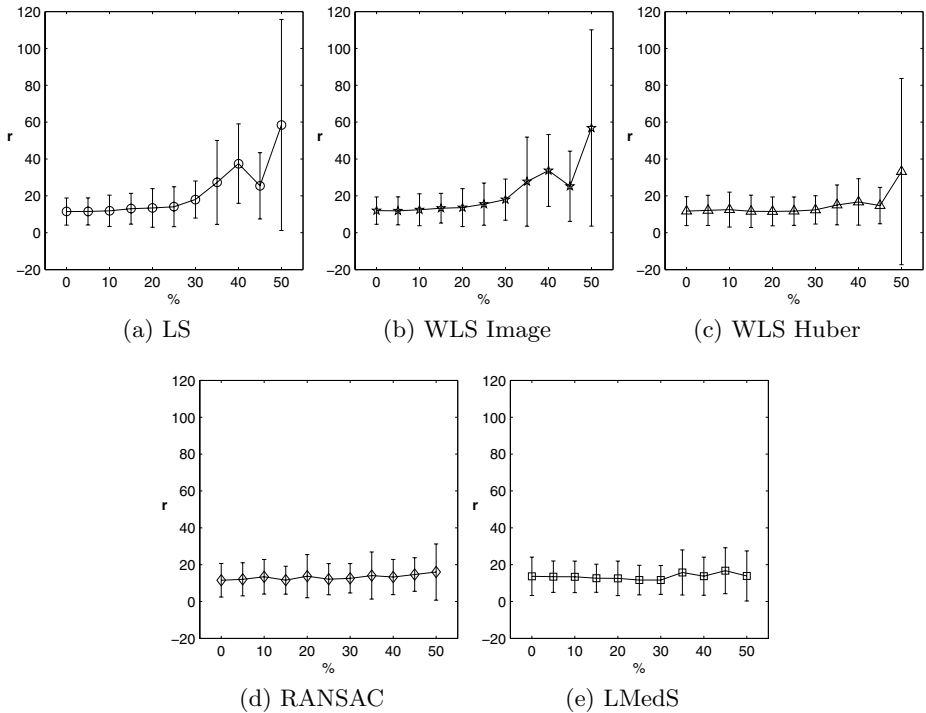


Fig. 5. Capillary Robustness. Mean residual r is plotted against initialisation outlier σ as a percentage of training set extent.

3.2 Outlier Tolerance

To investigate the effectiveness of the various parameter estimation methods under known conditions, models were fitted to data that had been perturbed by

non-Gaussian noise. Each annotation landmark in each data set was perturbed by Gaussian noise with standard deviation $\sigma = 0.5$ pixels. 30% of the landmarks in each annotation were selected at random and perturbed again by Gaussian noise with $\sigma = 50\%$ of the maximum extent of the training set annotations. Model parameters were estimated using each method and the residuals calculated between the original data and the model representation. WLS Image was not considered in this case. Figure 4 shows the mean residual for each set of data and each method, together with error bars of ± 1 standard deviation. In each case, the random sampling methods outperform LS and WLS Huber. This is as expected as studies have reported that WLS methods are only robust when less than 20 – 25% of the data is outlying [17]. It is noteworthy that the worst performance for WLS Huber is exhibited when applied to the capillary model, which has been constructed from highly variable shapes with little consistent structure. The model contains only weak constraints on capillary shape [9] which contributes to the poor WLS Huber performance.

3.3 ASM Robustness

To investigate the effects of robust parameter estimation on ASM search, a set of leave-one-out searches were performed. A subset of 10 images were selected at random from each set of data and a single iteration of ASM search was carried out on each. Each search was initiated from the position and parameters of the correct annotated boundary, distorted by applying Gaussian noise to the landmark positions and randomly creating outliers, as in section 3.2. In this case 10% of points were made outliers. The size of σ used to create the outlier set was varied between 0 and 50% of the training set extent. The final residuals between the model fit position and the annotation(s) were recorded. In the case of the multiple capillary annotations, the smallest residual for each model point in each image was used to form \bar{r} . Figures 5–7 show residual means and standard deviations for each set of data and method.

In each of the evaluations, the search gives comparable results when outlier distances are small. However, in each case the random sampling methods are much more robust in the presence of large outlying distances. WLS Huber estimation is more robust than the LS and WLS Image estimators, only breaking down when the outlier σ becomes large. LS and WLS Image estimators are approximately equivalent for each set of data. This suggests that there is no useful information in the quality of profile model matches to image data. In the case of capillary images it has previously been hypothesised that ‘good’ profile model matches are often found in inaccurate positions [9]. The similarity of LS and WLS Image supports this assumption.

3.4 ASM Accuracy

The utility of robust techniques in practical situations has been evaluated by performing a set of ASM searches. Models were fitted to the images used above

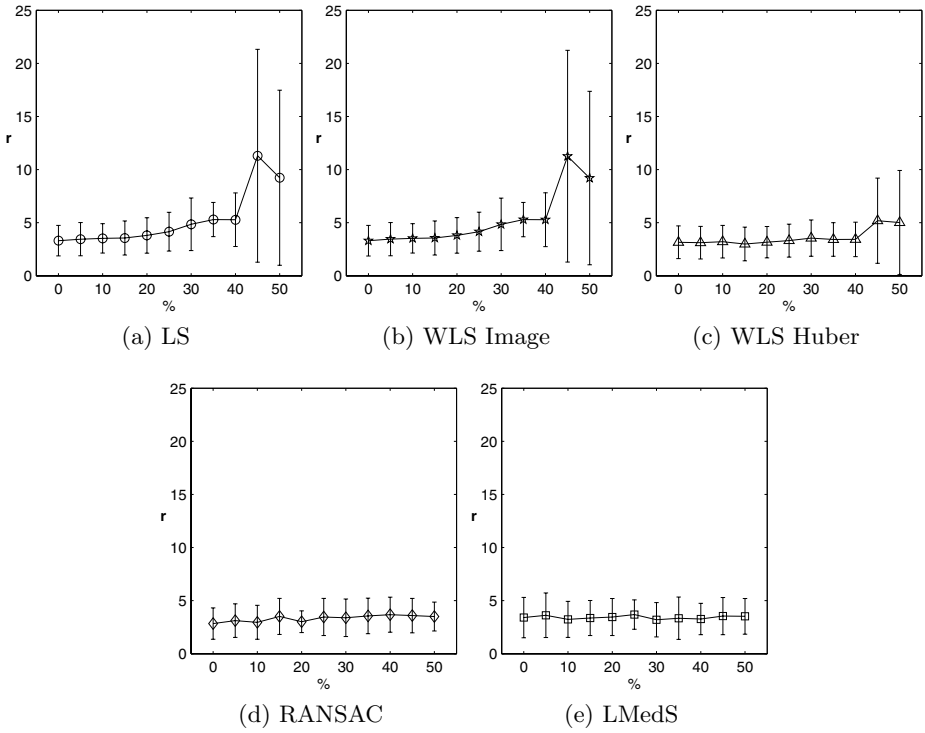


Fig. 6. Ventricle Robustness. Mean residual r is plotted against initialisation outlier σ as a percentage of training set extent.

using a single-resolution ASM search, initialised from the model mean shape and pose. Results from each set of data and each method are shown in Fig. 8.

In general, random sampling parameter estimation improves search accuracy and consistency compared to LS and WLS Image. This is shown well in prostate search results, where LMedS gives a reduction in average residual of 52%. Improvements in search accuracy using the weakly constrained capillary model are marginal. Capillary images contain many regions of locally confusing image evidence that consistently attract profile model matches. These areas can be seen as the light image regions outside of the annotations of the capillary images in Fig. 1. The constraints imposed by the capillary model are not sufficient to identify these matches as inconsistent with the global trend of all profile model matches. Because of this, random sampling and M-estimator robust parameter estimators do not identify the data as outlying and performance does not improve. In general, WLS Image does not provide a reliable scheme to improve search accuracy. In each set of searches the other robust estimators result in better search accuracy than WLS Image. The approach actually degrades search accuracy in capillary images, an effect caused by the regions of locally misleading evidence.

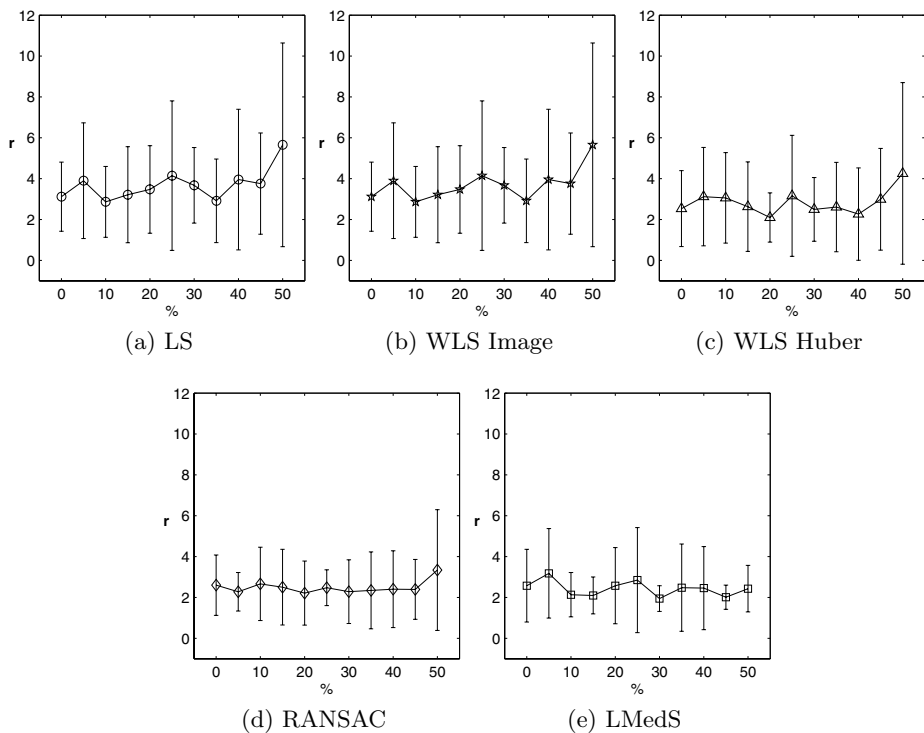


Fig. 7. Prostate Robustness. Mean residual r is plotted against initialisation outlier σ as a percentage of training set extent.

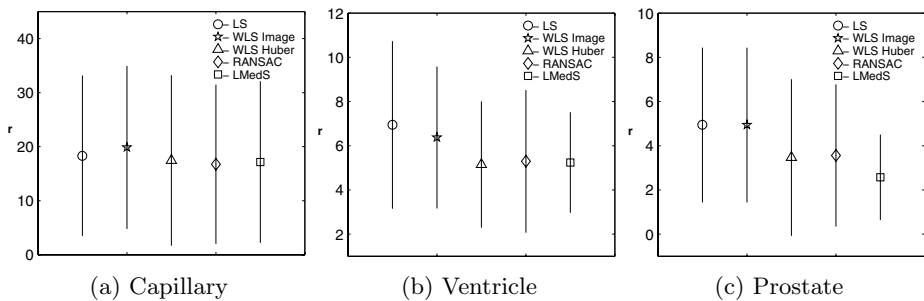


Fig. 8. ASM Search Accuracy. Mean residual r is plotted for each set of searches and each parameter estimation method. Error bars show ± 1 std. dev.

4 Conclusions

In many practical applications of shape model fitting, the assumption that residuals will have a Gaussian distribution will not be accurate. In particular, the presence of confusing evidence, due to noise, or highly variable image structure, produces “outliers” in the set of image points used to estimate the model parameters. We have evaluated four methods of parameter estimation intended to provide increased robustness to outliers in the fitting process, comparing these with the standard least squares approach. Two of the methods (RANSAC and LMedS) are examples of random sampling techniques. WLS Huber is a commonly used M-estimator. All three approaches gave improved robustness over the LS fit in the presence of synthetically generated outliers, the random sampling methods giving the best results. In general, the increased robustness results in increased search accuracy. This improvement is small in the case of capillary images because of the weakness of the constraints that can be imposed with models of capillary shape. The searches using WLS Image were intended to investigate the effect of reducing the influence in the fitting of points where the image data do not conform strongly to the local grey-level model. The hypothesis here is that most outliers occur because there is no strong image evidence in the local search area. Fitting should be improved if the influence of such data is reduced. The absence of any improvement using this technique indicates that outliers often occur because isolated points are found that correspond well to the model image patch.

The increased robustness of the random sampling and M-estimator methods is, of course, gained at the expense of increased computational cost.

Robust model parameterisation by itself is not a complete solution to the complex medical image analysis problems addressed in this paper. However, robust estimators have been shown to improve the robustness and accuracy of ASM search, and are potentially a useful modification to the standard ASM algorithm in many practical situations.

References

- [1] M. J. Black and A. D. Jepson. EigenTracking: Robust matching and tracking of articulated objects using a view-based representation. In *Proceedings of the European Conference on Computer Vision*, pages 329–342. Springer-Verlag, 1996.
- [2] A. Chauhan. The use of active shapes models for the segmentation of the prostate gland from magnetic resonance images. Master’s thesis, University of Manchester, 2001.
- [3] T. F. Cootes, C. J. Taylor, D. H. Cooper, and J. Graham. Active Shape Models - their training and application. *Computer Vision and Image Understanding*, 61(1):38–59, Jan. 1995.
- [4] M. A. Fischler and R. C. Bolles. Random Sample Consensus: A paradigm for model fitting with applications to image analysis and automated cartography. *Communications of the ACM*, 24(6):381–395, 1981.
- [5] J. P. Hampel, E. M. Ronchetti, P. J. Rousseeuw, and W. A. Stahel. *Robust Statistics: An Approach Based on Influence Functions*. Wiley, New York, 1986.

- [6] A. Hill, C. T. Taylor, and T. F. Cootes. Object recognition by flexible template matching using genetic algorithms. In *Proceedings of the 2nd European Conference on Computer Vision*, pages 852–856, Santa Margherita Ligure, Italy, May 1992.
- [7] P. J. Huber. *Robust Statistics*. Wiley, New York, 1981.
- [8] P. Meer, A. Mintz, and A. Rosenfeld. Robust regression methods for computer vision: A review. *International Journal of Computer Vision*, 6:59–70, 1991.
- [9] M. Rogers. *Exploiting Weak Constraints on Object Shape and Structure for Segmentation of 2-D Images*. PhD thesis, University of Manchester, 2001.
- [10] M. Rogers and J. Graham. Exploiting weak shape constraints to segment capillary images in microangiopathy. In *Proceedings of Medical Image Computing and Computer-Assisted Intervention*, pages 717–716, Pittsburg, USA, 2000.
- [11] P. J. Rousseeuw. Least median of squares regression. *Journal of the American Statistical Association*, 79:871–880, 1984.
- [12] P. J. Rousseeuw. *Robust Regression and Outlier Detection*. Wiley, New York, 1987.
- [13] S. Solloway, C. E. Hutchinson, J. C. Waterton, and C. J. Taylor. Quantification of articular cartilage from MR images using Active Shape Models. In B. Buxton and R. Cipolla, editors, *Proceedings of the 4th European Conference on Computer Vision*, volume 2, pages 400–411, Cambridge, England, April 1996. Springer-Verlag.
- [14] C. V. Stewart. MINPRAM, a new robust estimator for computer vision. *IEEE Transactions on Pattern Analysis and Machine Intelligence*, PAMI-17(10):925–938, 1995.
- [15] C. V. Stewart. Bias in robust estimation caused by discontinuities and multiple structures. *IEEE Transactions on Pattern Analysis and Machine Intelligence*, 19(8):818–833, Aug 1997.
- [16] H. H. Thodberg and A. Rosholm. Application of the Active Shape Model in a commercial medical device for bone densitometry. In T. F. Cootes and C. J. Taylor, editors, *Proceedings of the 12th British Machine Vision Conference*, volume 1, pages 43–52, September 2001.
- [17] P. H. S. Torr and D. W. Murray. The development and comparison of robust methods for estimating the fundamental matrix. *International Journal of Computer Vision*, 24(3):271–300, 1997.
- [18] P. H. S. Torr and A. Zisserman. MLESAC: A new robust estimator with application to estimating image geometry. *Computer Vision and Image Understanding*, 78(1):138–156, April 2000.
- [19] Z. Zhang. Parameter estimation techniques: A tutorial with application to conic fitting. *Image and Vision Computing*, 15:59–76, 1997.
- [20] Z. Zhang, R. Deriche, O. Faugeras, and Q.-T. Luong. A robust technique for matching two uncalibrated images through the recovery of the unknown epipolar geometry. *Artificial Intelligence Journal*, 78:87–119, October 1995.